Journal of Thermal Analysis and Calorimetry, Vol. 58 (1999) 663-669

EFFECT OF THE HEATING RATE ON CRYSTALLIZATION KINETICS OF $Mg_{84}Ni_{12.5}Y_{3.5}$ AMORPHOUS RIBBONS

E. Korin[1*], *L. Soifer*[1], *D. Mogiliyanskii*[1], *Ya. Soifer*[2], *I. Brodova*[3] *and A. Manuhin*[3]

[1]Department of Chemical Engineering, Ben-Gurion University of the Negev, P.O. Box 653 Beer-Sheva 84105, Israel
[2]Institute of Solid State Physics, Chernogolovka 142432
[3]Institute of Metals Physics, Kovalevskaya Str. 18, Ekaterinburg 620219, Russia

(Received June 2, 1998; in revised form January 16, 1999)

Abstract

Crystallization kinetics of $Mg_{84}Ni_{12.5}Y_{3.5}$ amorphous ribbons produced by the melt-spinning method, was studied by DSC analysis and X-ray diffraction. The effect of heating rate (from 2 to 240 K min^{-1}) was investigated in the temperature range from 298 to 673 K. The results showed that the crystallization process took place in two stages: a) crystallization of part of the amorphous matrix to an intermediate phase and hcp-Mg, and b) transformation of the intermediate phase and the remaining amorphous material to Mg_2Ni+Mg (solid solution of Y in Mg). Increasing the heating rate from 2 to 240 K min^{-1} results in increases of the temperature difference between the two-step crystallization of the first stage transformation processes from 33 to 56 K and in increases of the temperature difference between the two-stage transformation from 62 to 97 K.

Keywords: crystallization kinetics, intermediate nanocrystal phase, Mg–Ni–Y amorphous ribbons

Introduction

Mg-based amorphous alloys have the unique feature of combining relatively high mechanical strength, hydrogen storage ability with low specific density. Furthermore, mechanical properties [1] and hydrogen storage ability [2] may be higher in mixed-phase alloys, in which nanocrystalline particles are dispersed in the amorphous matrix. The superiority of mixed-phase alloys over amorphous alloys with the same composition depends on the size and the interparticle distance. The desirable microstructure of the alloys could be obtained by controlling the operation conditions at the production process or by thermal treatment for partial crystallization of

* Author to whom all correspondence should be addressed.

1418–2874/99/ $ 5.00

Akadémiai Kiadó, Budapest
Kluwer Academic Publishers, Dordrecht

the amorphous alloys. In both cases, crystallization kinetics data for the specific amorphous alloys is of utmost importance. Experimental studies indicate that in several specific alloys, such as Mg–Zn–La [3], Mg–Zn–Ce [4] and Mg–Ni–Ca [5], at a concentration of the rare earth or alkaline earth metal of ~2–3 at%, the crystallization process occurs in two stages according to the following transformation processes: amorphous matrix→intermediate nanostructured phase+Mg+remaining amorphous matrix→intermetallic compounds+Mg. Among the Mg-based amorphous alloys the Mg–Ni–Y has the higher mechanical properties [1] (Inoue *et al.*, 1993). Most of the published results on crystallization studies of Mg–Ni–Y alloys [1] has been related to compositions above 5% Y. In these studies no intermediate nanostructured phase has been observed, although it exists in the binary system: Mg–Ni (as mentioned by [1]). Considering that it exists lean alkaline-earth-metal, $Mg_{82.5}Ni_{15}Ca_{2.5}$ alloys, it is expected that similar behavior occurs in lean Y (less than 5%) Mg–Ni–Y alloys. Recently, experimental results related to Mg–Ni–Y alloys with composition $Mg_{87}Ni_{12.5}Y_{1.5}$ [6], $Mg_{84}Ni_{12.5}Y_{3.5}$ [7, 8] and $Mg_{80}Ni_{15}Y_{3.5}$ [9] showed that the intermediate nanostructured phase forms also in crystallization processes of these amorphous alloys by thermal treatments. However, no systematic crystallization kinetics data related to Y lean MgNi based amorphous alloys have been published.

This work presents experimental studies on the crystallization kinetics of Y lean MgNi based amorphous ribbons produced by the melt-spinning technique. The paper focuses on the effect of heating rate on the crystallization kinetics.

Experimental

$Mg_{84}Ni_{l2.5}Y_{3.5}$ amorphous ribbons with a cross-section of 0.02×2 mm were prepared by the following procedure: A master alloy of the desirable atomic ratio was prepared by an induction melting method from a mixture of pure magnesium (99.99), pure nickel (99.99) and pure yttrium (99.9 mass%). The mixture was maintained under vacuum in an alumina (Al_2O_3) crucible, covered with a KCl–NaCl slag-cover, and soaked for 30 min at a temperature of 1073 K. A solid ingot was produced by slow cooling of the melted alloy. The ingot was remelted under an Ar atmosphere at 933 K, soaked for 5 min, and then used to produce the amorphous ribbons by a melt-spinning technique. DSC analyses of 4–5 mg samples were performed by Mettler Toledo DSC 820 System. The instrument was calibrated with pure indium (melting temperature 429.9 K, heat of fusion 28.4 J g^{-1}). The analyses were performed in an Al crucible under a nitrogen atmosphere (99.9% pure) at heating rates of 2, 4, 8, 15, 30, 60, 120 and 240 K min^{-1} in a temperature range of 298 to 673 K. The structures of the phases were determined by X-ray diffraction with a PW 1050/70 Philips X-ray Diffractometer with CuK_α radiation at a constant temperature of 298±1 K.

The specimens from the ribbons at different stages of the DSC analyses were examined. The specimens were quenched in an oil bath to reduce the effect of transit cooling time of the specimens.

Results and discussion

DSC analysis and X-ray diffraction were used to study the effect of heating rate on the crystallization kinetics of amorphous ribbons of $Mg_{84}Ni_{12.5}Y_{3.5}$. Representative DSC curves for heating rates of 2 ,8, 30 and 120 K min^{-1} are shown in Fig. 1. Five exothermic peaks were observed. Figure 2 shows the X-ray diffraction patterns for a $Mg_{84}Ni_{12.5}Y_{3.5}$ ribbon that was heated to 443, 473, 533, 583 and 643 K, temperatures related to the peaks observed in the DSC curve for a heating rate of 30 K min^{-1}. The broad halos of the diffractogram obtained before DSC analysis indicate the amorphous structure of the $Mg_{84}Ni_{12.5}Y_{3.5}$ ribbon. The similar broad diffraction effect obtained at 443 and 473 K indicate that the amorphous structure is quite stable at 473 K. The diffractogram obtained at 533 K exhibited three peaks at 2θ=21.7, 37.0 and 38.1°, respectively. Considering that the X-ray diffractogram of crystalline Mg has a peak at 2θ=36.619°, which corresponds to the (101) plane [10], one can assume that the peak at 37.0° may be attributed to crystalline Mg, the slight difference in values resulting from the solid solution of Y in the Mg. The two other peaks (2θ=21.7 and 38.1° could not be attributed to any known crystalline phase in the ternary Mg–Ni–Y system. For the sample heated to 583 K, two additional weak peaks at 2θ=20.1 and 34.5° were observed, these are likely to correspond to Mg and Mg_2Ni crystalline phases [10].

Finally, the sample heated to 643 K shows that enhancement of the peaks corresponding to Mg and Mg_2Ni were enhanced and only traces of the peaks relating to the undefined crystalline phase remained. This indicates that in the heating step be-

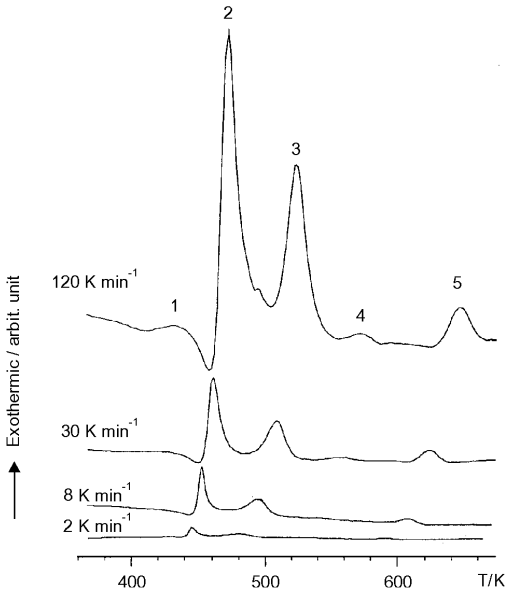

Fig. 1 Representative DSC curves of the amorphous ribbons $Mg_{86}Ni_{12.5}Y_{1.5}$ at heating rate of 2, 8, 30 and 120 K min^{-1}, respectively. Five exothermic peaks (designated P1-P5) are evident for each curve

tween 583 to 643 K the undefined crystalline phase and the remaining amorphous phases are transformed into Mg (a solid solution of Y in Mg) and Mg_2Ni. The absence in the diffractograms of peaks corresponding to yttrium or yttrium compounds indicates that the yttrium is dissolved in Mg or Mg_2Ni.

The X-ray diffraction results indicated that the small and broad first DSC peak could be related to the irreversible structural relaxation, and the sharp decreases in the DSC curve were due to the glass transition. The sharp exothermic double DSC peak (designated 2 and 3 on Fig. 1) was due to first stage crystallization: precipitation of an intermediate unknown phase and the smaller fourth and fifth exothermic DSC peaks reflected the second stage of crystallization (i.e., transformation of the remaining amorphous matrix and the undefined crystalline phase to the stable phase i.e., Mg, Mg_2Ni and a solid solution of Y in Mg (or Mg_2Ni). In general, in cases in which there is overlap of DSC peaks in the crystallization of an amorphous alloy and the values of the activation energies are in the range of 273 and 196 kJ mol^{-1}, the peaks may be attributed to nucleation and crystal growth, respectively [11].

Based on the characteristic temperatures of the DSC curves (Fig. 1) and the X-ray patterns (Fig. 2), Table 1 summarizes the effect of a heating rate on the following parameters: the temperature of the first stage of crystallization (T_x), the temperature of the second stage of crystallization (T_{cr}), the temperature difference between T_x and T_{cr}($\Delta T_{cr}=T_x-T_{cr}$), the total heat of crystallization for the first stage (ΔH_2), the heat of crystallization related to the growth for first stage of crystallization (ΔH_3), the ratio between heat of the growth for first stage of crystallization to the total heat of the growth for first stage of crystallization ($\Delta H_3/\Delta H_2$), the temperatures of maxi-

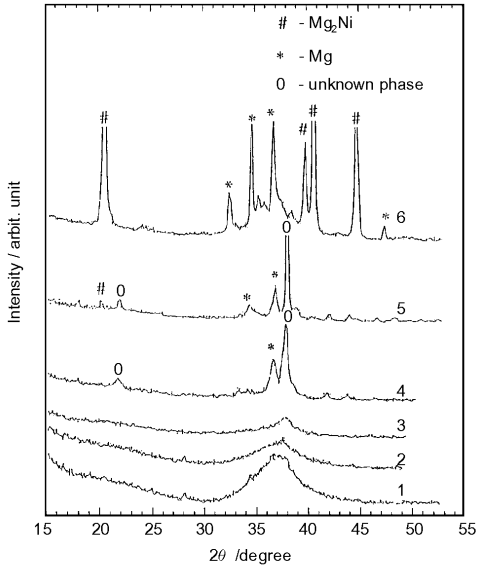

Fig. 2 X-ray diffraction patterns of melt-spun ribbon before heating and after heating up to 443, 473, 533, 583 and 643 K (curve 2 to 6 respectively). Curve 1 was obtained at 298 K, i.e. as obtained from the quenching

Table 1 Effect of heating rate (β) on characteristic parameters of the DSC curves for $Mg_{84}Ni_{12.5}Y_{3.5}$ amophous ribbons

β/	T_x/	T_{cr}/	ΔT_{cr}/	ΔH_2/	ΔH_3/	$\Delta H_3/\Delta H_2$	T_{p2}/	T_{p3}/	ΔT_p/
K min^{-1}		K		J g^{-1}				K	
2	438	500	62	76.5	24.0	0.31	447	480	33
4	443	528	85	79.3	21.4	0.27	448	486	38
8	446	530	84	83.2	23.9	0.28	451	493	42
15	448	532	84	93.3	23.6	0.25	455	501	46
30	450	538	88	77.5	23.8	0.27	460	508	48
60	453	550	97	88.0	26.3	0.30	464	514	50
120	468	553	85	79.3	22.8	0.29	470	522	52
240	459	–	–	75.4	24.5	0.32	473	529	56

T_x – temperature of the first stage of crystallization, T_{cr} – temperature of the second stage of crystallization, T_{p2} – temperature of maximum of the second DSC peak, T_{p3} – temperature of maximum of the third DSC peak, $\Delta T_x=T_g-T_x$, $\Delta T_{cr}=T_x-T_{cr}$, ΔT_p – temperature difference between T_{p3} and T_{p2}, ΔH_2 – heat of first stage of the crystallization, ΔH_3 – heat of the growth for first stage of crystallization, $\Delta H_3/\Delta H_2$ – ratio between heat of the growth for first stage of crystallization and heat of the growth for first stage of crystallization

mum of the second (T_{p2}) and third (T_{p3}) DSC peaks and the temperature difference between T_{p3} and T_{p2} ($\Delta T_p=T_{p3}-T_{p2}$).

The increase in heating rate from 2 to 240 K min^{-1} resulted in an increase the value for ΔT_p were from 33 and 560 K. This value of ΔT_p was well above of that ~16 K, as reported for amorphous $Mg_{82.5}Ni_{15}Ca_{2.5}$ and $Mg_{72}Zn_{25}La_3$ alloys (at a heating rate of 40 K min^{-1}). The result shows that both the total heat of the crystal-

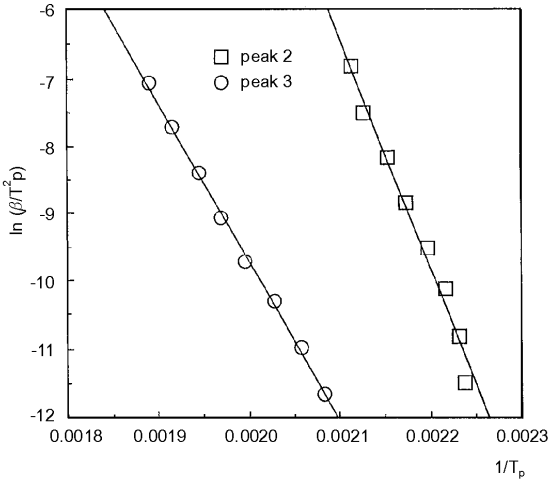

Fig. 3 Kissinger plot: $\ln(\beta / T_p^2)$ *vs.* $1/T_p$, where T_p is the peak temperature and β is the heating rate

lization of the first stage (ΔH_2) and the ratio $\Delta H_3/\Delta H_2$ are practically independent of the heating rate.

The apparent activation energies for the crystallization processes were estimated by the Kissinger 'peak shift' method. Plots of $\ln(\beta / T_p^2)$ *vs.* $1/T_p$, are presented in Fig. 3, where T_p – the peak temperature and β – the heating rate. The activation energies calculated from the slopes of the fitted linear functions for nucleation and crystal growth of the first crystallization stage were : 286±10 and 195±10 kJ mol^{-1}.

From the XRD patterns, the average crystal sizes of the intermediate unknown phase was determined by Scherrer's equation [12]. The sample heated to 583 K presented unknown phase crystals and Mg nanocrystals of 10 nm in size. The temperature span between T_{p3} and T_{p2} ($\Delta T_p=T_{p3}-T_{p2}$) and the temperature span between T_{cr}($\Delta T_{cr}=T_x-T_{cr}$), indicated high thermal stability of the nanoscale intermediate unknown phase+Mg and remaining amorphous matrices.

Conclusions

The present experimental study on the crystallization kinetics of $Mg_{84}Ni_{12.5}Y_{3.5}$ amorphous ribbons produced by the melt-spinning technique are summarized as follows:

l. The crystallization of $Mg_{84}Ni_{12.5}Y_{3.5}$ amorphous ribbon was found to occur in two steps: amorphous matrix→intermediate nanostructured phase+Mg (solid solution of Y in the Mg)+remaining amorphous matrix→Mg_2Ni+Mg (solid solution of Y in Mg). This result is similar to the crystallization kinetic mechanism for several other Mg-based alloys reported in the literature (Mg–Zn–La, Mg–Zn–Ce and Mg–Ni–Ca).

2. The DSC curves shows that first crystallization stage is characterized by two steps; one related to nucleation and the second to crystal growth. The calculated apparent activation energies for nucleation and crystal growth are 286±10 and 195±10 kJ mol^{-1}, respectively.

3. The average crystal sizes of the intermediate unknown phase was estimated to be 10 nm in size.

4. Increases the heating rate from 2 to 240 K min^{-1} results in increases of the temperature difference between the two steps crystallization of the first stages transformation processes from 33 to 56 K and in increases of the temperature difference between the two stages transformation from 62 to 97 K. This indicates the possibility for tailoring the heating treatment to produce the required fraction of the amorphous phase.

References

1 A. Inoue and T. Masumoto, Mater. Sci. Eng., A 173 (1993) l.
2 S. Orimo, K. Ikeda, H. Fujii et al., Acta Mater., 45 (1997) 2271.
3 A. Inoue, N. Nishiyama, S. G. Kim and T. Masumoto, Mater. Trans. J I M, 33 (1992) 360.
4 S. G. Kim, A. Inoue and T. Masumoto, Mater. Trans. J I M, 32 (1991) 8725.
5 T. Shibata, A. Inoue and T. Masumoto, J. Mater. Sci., 28 (1993) 379.

6 Ya. Soifer, N. P. Kobelev, E. Korin, L. Soifer and I. Brodova, 'MAGNESIUM 97, The First Israeli International Conference on Magnesium Science & Technology', Abstract, Dead Sea, Israel 1997, p. 88.
7 E. Korin, L. Soifer, D. Mogylianskii, A. Manukhin, I. Brodova and Ya. Soifer 'MAGNESIUM 97, The First Israeli International Conference on Magnesium Science & Technology', Abstract, Dead Sea, Israel 1997, p. 74.
8 Ya. Soifer, N. P. Kobelev, I. Brodova, A. Manukhin, E. Korin and L. Soifer, Internal friction and the Young's modulus change associated with amorphous to nanocrystalline phase transition in Mg–Ni–Y alloys. NANO '98 Fourth international Conference on Nanostructured Materials, Abstract, Part 2, Stockholm Sweden, 1998, p.121.
9 I. G. Brodova, A. B. Manukhin and A. S. Bykov, Phys. Met. and Metallograf., 85 (1998) 355.
10 W. F. McClune, Powder Diffraction File. Alphabetical Index of the Inorganic Phases, International Center for Diffraction Data, Pennsylvania, USA 1984.
11 L. Batterazatti, M. Barrico and C. Antonione, J. Alloys and Comp., 209 (1994) 341.
12 H. P. Klug and L. F. Alexander, X-ray Diffraction Procedures. Wiltey Inter. Science Publ., New York 1974.